Journal of Alloys and Compounds 509 (2011) 4871–4874

Contents lists available at ScienceDirect

Journal of Alloys and Compounds

journal homepage: www.elsevier.com/locate/jallcom

Luminescent properties of UV excitable blue emitting phosphors $MSr_4(BO_3)_3:Ce^{3+}$ (M = Li and Na)

Chongfeng Guo[a,b], Xu Ding[b], Hyo Jin Seo[c,*], Zhaoyu Ren[a], Jintao Bai[a]

[a] National Key Laboratory of Photoelectric Technology and Functional Materials (Culture Base) in Shaanxi Province, National Photoelectric Technology and Functional Materials & Application of Science and Technology International Cooperation Base, Institute of Photonics & Photon-Technology and Department of Physics, Northwest University, Xi'an 710069, PR China

[b] Wuhan National Laboratory for Optoelectronics, Huazhong University of Science and Technology, Hubei Province, Wuhan 430074, PR China

[c] Department of Physics, Pukyong National University, Busan 608-737, Republic of Korea

ARTICLE INFO

Article history:
Received 3 November 2010
Received in revised form 27 January 2011
Accepted 27 January 2011
Available online 22 February 2011

PACS:
78.20.–e
78.55.–m

Keywords:
Phosphor
Borate
Luminescence

ABSTRACT

A series of Ce^{3+} doped novel borate phosphors $MSr_4(BO_3)_3$ (M = Li or Na) were successfully synthesized by traditional solid-state reaction. The crystal structures and the phase purities of samples were characterized by powder X-ray diffraction. The optimal concentrations of dopant Ce^{3+} ions in compound $MSr_4(BO_3)_3$ (M = Li or Na) were determined through the measurements of photoluminescence spectra of phosphors. Ce^{3+} doped phosphors $MSr_4(BO_3)_3$ (M = Li or Na) show strong broad band absorption in UV spectral region and bright blue emission under the excitation of 345 nm light. In addition, the temperature dependences of emission spectra of $M_{1+x}Sr_{4-2x}Ce_x(BO_3)_3$ (M = Li or Na) phosphors with optimal composition $x = 0.05$ for Li and $x = 0.09$ for Na excited under 355 nm pulse laser were also investigated. The experimental results indicate that the $M_{1+x}Sr_{4-2x}Ce_x(BO_3)_3$ (M = Li or Na) phosphors are promising blue emitting phosphors pumped by UV light.

1. Introduction

In the last few years, white light emitting diodes (*w*-LEDs) have begun replacing incandescent and fluorescent lights in a number of niche applications due to their advantages in energy saving, related environmental benefits, and the steadily dropping cost [1–3]. Currently, most commercially available *w*-LED products in the market are fabricated by coating a layer of yellow emitting phosphor YAG:Ce $[(Y_{1-a}Gd_a)_3(Al_{1-b}Ga_b)_5O_{12}:Ce^{3+}]$ on blue LED chips, which suffers from a poor color rendering index ($Ra < 80$) and high color temperature ($T_c > 4500$ K) due to the deficiency of the green and red light [4]. In order to overcome these drawbacks, three-band *w*-LEDs with high *Ra* and the tunable color temperature were proposed by pumping tricolor (red–green–blue) phosphors with near-UV LED chips, which is based on the working mechanism of fluorescent lamps [5]. Though tricolor phosphors used for fluorescent lamp have been investigated in detail, the present tricolor emitting phosphors could not be efficiently excited by near-UV light. It is an urgent task to hunt for some novel tricolor phosphors those can be excited by near-UV light and emit required visible light. For the phosphors used in near-UV white LEDs, the basically requirements are strong absorption in the near-UV range and high conversion efficiency. Moreover, high chemical and physical stabilities are also important for improving the lifetimes of *w*-LEDs [6].

Up to now, $BaMgAl_{10}O_{17}:Eu^{2+}$ ($BAM:Eu^{2+}$) is still regarded as the preferred blue-emitting phosphor for white light emitting diodes based on the near-UV LED. However, the synthesis of $BAM:Eu^{2+}$ is usually at temperature as high as 1300–1600 °C for several hours, which leads to the increase of *w*-LEDs cost [7]. It is necessary to search for a new blue phosphor with low cost and efficient blue emission excited in the near-UV range. As an important family of luminescent material host, borate has attracted much attention not only owing to its excellent thermal stability, environmental benignity, and potential low-cost synthesis, but also a number of compounds with different structures can be selected [8]. Novel cubic borates $MSr_4(BO_3)_3$ (M = Li or Na) have been firstly synthesized by Wu, but there are few reports on the luminescent properties of rare earth ions doped these compounds [9,10]. Among rare earth ions, Ce^{3+} is an efficient activator for the phosphors applied in the field of lighting because the luminescence color of the Ce^{3+} doped phosphor can be tuned from red to UV region, which due to the 5*d* energetic position of Ce^{3+} is sensitive to the host lattice [11,12]. In this work, photoluminescent properties of Ce^{3+} doped $MSr_4(BO_3)_3$ (M = Li or Na) were investigated in detail, which exhibits bright blue emission under the excitation of UV light.

* Corresponding author.
E-mail addresses: gcfzsu@yahoo.com.cn, hjseo@pknu.ac.kr (H.J. Seo).

0925-8388/$ – see front matter © 2011 Elsevier B.V. All rights reserved.
doi:10.1016/j.jallcom.2011.01.194

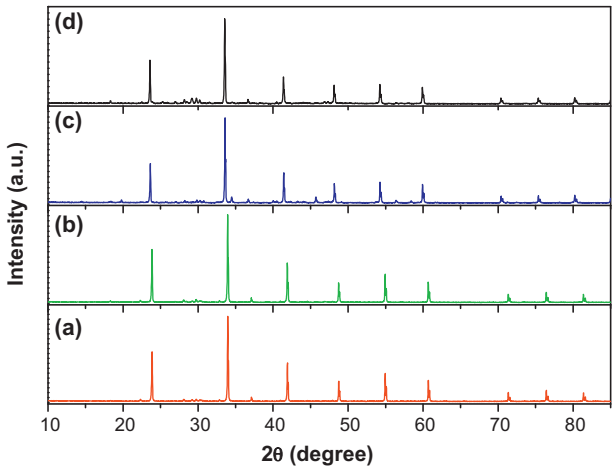

Fig. 1. XRD patterns of samples $LiSr_4(BO_3)_3$ (a), $Li_{1.05}Sr_{3.9}Ce_{0.05}(BO_3)_3$ (b), $NaSr_4(BO_3)_3$ (c) and $Na_{1.09}Sr_{3.82}Ce_{0.09}(BO_3)_3$ (d).

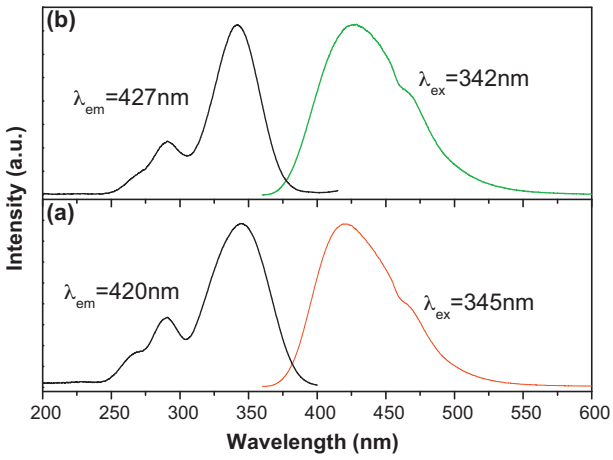

Fig. 2. PLE and PL spectra of $Li_{1.05}Sr_{3.9}Ce_{0.05}(BO_3)_3$ (a) and $Na_{1.09}Sr_{3.82}Ce_{0.09}(BO_3)_3$ (b).

2. Experimental

Polycrystalline powder samples were prepared by a solid-state reaction technique at high temperature and CO reducing atmosphere. Raw materials include $SrCO_3$, Li_2CO_3, Na_2CO_3, H_3BO_3 (3 mol% in excess to compensate for evaporation) and CeO_2, all starting materials were analytical grade. Considering the size of Sr^{2+} radius, it is believed that the doping ions Ce^{3+} are expected to occupy the Sr^{2+} crystallographic sites rather than the Li^+ or Na^+ sites in $MSr_4(BO_3)_3$ (M = Li or Na) crystal cells. Additionally, apart from the size effect, a larger valence difference between Ce^{3+} and Li^+ is also not favorable for Ce^{3+} replacement of Li^+, as observed in Li_2SrSiO_4:Ce^{3+} [13]. The excessive Li_2CO_3 or Na_2CO_3 was used as charge compensator in $LiSr_4(BO_3)_3$ and $NaSr_4(BO_3)_3$, respectively, in order to maintain charge neutrality of the crystal. Therefore, the nominal composition of present samples are $M_{1+x}Sr_{4-2x}Ce_x(BO_3)_3$ (M = Li or Na). For the preparation of the present phosphors, stoichiometric amounts of raw materials with the nominal composition were intimately mixed and placed in a small covered corundum crucible. Then the small crucible was placed in a large outer crucible and buried in carbon sticks in order to reduce Ce^{4+} to Ce^{3+}. Afterwards, the large crucible with its contents was placed in a muffle furnace under ambient atmospheres and fired at 750 °C for 8 h. The commercial blue phosphor BAM:Eu^{2+} was purchased from NICHIA Corporation (Japan).

The structure and phase purity of sintered samples were identified by powder X-ray diffraction (XRD) analysis using an X'Pert PRO advanced automatic diffractometer with Cu-Kα radiation operated at 40 kV and 40 mA. The measurements of photoluminescence (PL) and photoluminescence excitation (PLE) spectra were carried out using a JASCO FP-6500 fluorescence spectrophotometer equipped with a 150 W xenon lamp as the excitation light source. PL spectra of all samples were tested three times to reduce the error. Their PL properties at higher temperature were evaluated using the same spectrophotometer with a homemade heating cell under the excitation of 355 nm pulsed laser. To eliminate the second-order emission of the source radiation, a cut-off filter was used in the process of measurement.

3. Results and discussion

The diffraction pattern is usually used to identify the crystal structure and the phase purity of sample. Fig. 1 shows the XRD patterns of samples $MSr_4(BO_3)_3$ (M = Li or Na) with and without dopants sintered at 750 °C for 8 h in the CO reducing atmosphere. In this study, concentration of Ce^{3+} is varied from $x = 0$ to 0.11, and the XRD patterns of all samples are similar. Here, only XRD patterns of samples $Li_{1.05}Sr_{3.9}Ce_{0.05}(BO_3)_3$ and $Na_{1.09}Sr_{3.82}Ce_{0.09}(BO_3)_3$ are displayed as representatives. As shown in Fig. 1, all of the diffraction peaks are in good agreement with those of $MSr_4(BO_3)_3$ (M = Li or Na) in Ref. [9] and no detectable impurity phase is observed. This result illuminates that all these samples show similar crystal structures and the introduction of dopants does not cause any significant changes in the host structure, and the Sr^{2+} ions can be partially replaced by Ce^{3+} without change of crystalline structure. Comparing XRD patterns of $LiSr_4(BO_3)_3$ and $NaSr_4(BO_3)_3$, it is clearly observed that the two samples adopt cubic structure and are iso-structural. However, a slight shift in 2θ value towards the lower angle is found with completely substitution of Li^+ by Na^+, since the size of Na^+ (0.95 Å) is larger than that of Li^+ (0.60 Å) [14].

Ce^{3+} doped $MSr_4(BO_3)_3$ (M = Li or Na) phosphors show blue emission at room temperature under the excitation of UV light. The PLE and PL spectra of phosphors $Li_{1.05}Sr_{3.9}Ce_{0.05}(BO_3)_3$ and $Na_{1.09}Sr_{3.82}Ce_{0.09}(BO_3)_3$ are presented in Fig. 2(a) and (b), respectively. The excitation spectra of the samples (monitored at 420 nm for the former and 427 nm for the latter) are broad, and cover the spectral region from 200 to 400 nm. It can be seen that the excitation spectra consist of three broad bands with peaks at about 265, 290 and 345 nm (342 nm for M = Na), respectively, which are ascribed to the crystal field splitting of Ce^{3+} 5*d* orbits [15]. The emission spectra of the samples shows a broad asymmetric blue emission band with a maximum at 420 and 427 nm for $LiSr_4(BO_3)_3$ and $NaSr_4(BO_3)_3$ under the UV excitation, respectively, which are attributed to the $4f^0\,5d^1$–$4f^1$ ($^2F_{5/2}$ and $^2F_{7/2}$) transitions of Ce^{3+}. The Stokes shift can be roughly estimated by assuming that the excitation band is the mirror image of the emission band. Therefore, the Stokes shifts of $Li_{1.05}Sr_{3.9}Ce_{0.05}(BO_3)_3$ and $Na_{1.09}Sr_{3.82}Ce_{0.09}(BO_3)_3$ are calculated as about 5175 and 5820 cm^{-1}, respectively [16]. In addition, there is a minor red shift for the emission wavelength of Ce^{3+} in the compound $NaSr_4(BO_3)_3$ in comparison with that of Ce^{3+} in $LiSr_4(BO_3)_3$ compound, which can be understood in terms of the crystal field theory with the substitution of Li^+ by Na^+ [17].

The ground state configuration of the Ce^{3+} ($4f^1$) ion yields two levels, viz. $^2F_{5/2}$ and $^2F_{7/2}$, thus the emission spectrum of Ce^{3+} in one specific lattice site usually shows a typical double-band shape and the energy difference between the two bands is about 2000 cm^{-1}. In the compounds $MSr_4(BO_3)_3$ (M = Li or Na), there are two different crystallographical sites for Sr atoms. The Sr (1) atoms are coordinated to six oxygen atoms, forming distorted octahedral, while the Sr (2) atoms are eight-coordinated to oxygen atoms, forming two-capped trigonal prisms and sharing planes and edges with the adjacent $Sr(2)O_8$ polyhedra and $Sr(1)O_6$ octahedra, respectively [9]. For the Ce^{3+} doped compounds $MSr_4(BO_3)_3$ (M = Li or Na), Ce^{3+} ions are proposed to enter the Sr^{2+} sites, thus it is reasonable for Ce^{3+} to occupy two different Sr^{2+} sites. To analyze the asymmetric emission spectra, Gaussian peak fitting was carried out. Fig. 3 shows Gaussian curve fitting of the emission spectra those could be de-convoluted into four Gaussian peaks those are bands I(408 and 409 nm), II(446 and 453 nm), III(431 and 433 nm), and IV(479 and 480 nm) in $LiSr_4(BO_3)_3$ and $NaSr_4(BO_3)_3$, respectively. Bands I and II come from the emission of Ce^{3+} at one specific site referred to Ce (1); and the bands III and IV are attributed to the emission of the other Ce^{3+} center, named as Ce (2). The energy gap between the

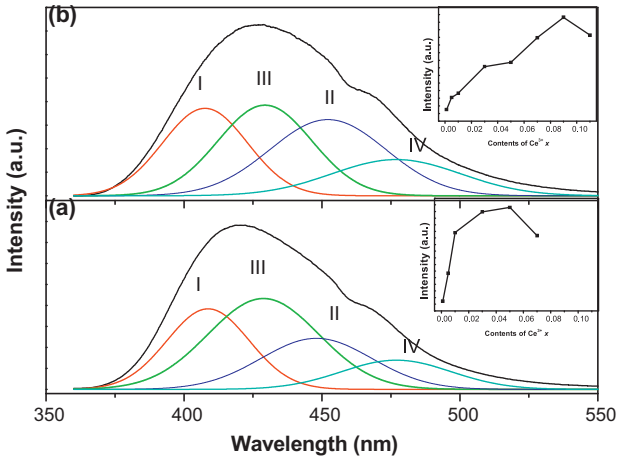

Fig. 3. Emission spectra of $Li_{1.05}Sr_{3.9}Ce_{0.05}(BO_3)_3$ (a) and $Na_{1.09}Sr_{3.82}Ce_{0.09}(BO_3)_3$ (b) excited at 345 nm at RT with four deconvoluted Gaussian peaks. Inset: the dependence of PL intensity on the concentrations of Ce^{3+}.

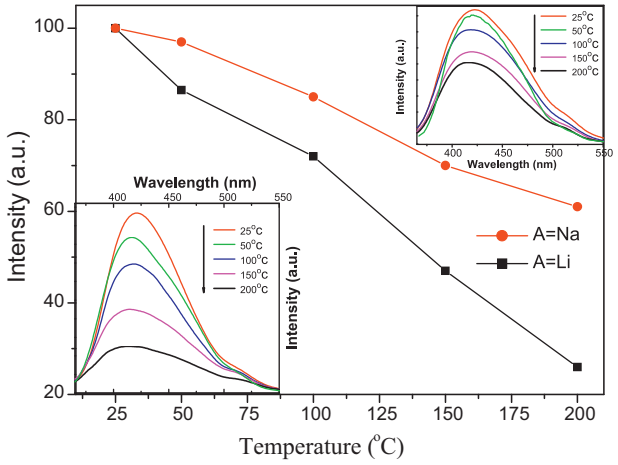

Fig. 4. The dependence of the normalized PL intensities of $Li_{1.05}Sr_{3.9}Ce_{0.05}(BO_3)_3$ (a) and $Na_{1.09}Sr_{3.82}Ce_{0.09}(BO_3)_3$ on temperature. Inset: the dependence of PL spectra of phosphor with optimal composition on temperature excited by 355 nm pulse laser.

bands I and II or the bands III and IV is close to 2000 cm^{-1} in the two samples, which is in agreement with the spin orbit splitting between the two ^2F multiplets of the Ce^{3+} ground state. The center Ce (1) is proposed to occupy the site of Sr (1) with a weaker crystal field, whereas the other center Ce (2) can be due to enter the sites of Sr (2) with a stronger crystal field [18]. Because the energy position of the lowest Ce^{3+} $5d^1$ level can be controlled by modifying the crystal strength that depends on site size, coordination environment, and so on. For the same cations, the large anion coordination number will lead to the strong crystal field strength, thus the crystal field splitting will generally increase. Therefore, the emission of Ce (2) should have a red-shift in comparison with that of Ce (1) and Ce (2) occupy the site of Sr (2), where eight O^{2-} anion coordinated one Sr^{2+} [19].

Insets of Fig. 2(a) and (b) show the dependences of $M_{1+x}Sr_{4-2x}Ce_x(BO_3)_3$ (M = Li or Na) phosphors PL intensities (defined as the integrated area intensities in the range of 365–550 nm) on the concentrations of Ce^{3+} (x) dopant. With increasing Ce^{3+} concentration, the intensity of the blue emission increases and reaches a maximum at about 5 at.% in $LiSr_4(BO_3)_3$ and 9 at.% in $NaSr_4(BO_3)_3$. Above this concentration, the intensity of the blue emission decreases. It is believed to be the shorter and shorter distance between Ce^{3+} ions with increasing concentration that introduced the concentration quenching. The concentration quenching phenomena will not occur if the average distance between the identical Ce^{3+} ions is so large that the energy migration is hampered, thus the critical distance is an important parameter which can be estimated from geometrical consideration with help of the following formula [20]:

$$R_c \approx 2\left(\frac{3V}{4\pi x_c N}\right)^{1/3} \quad (1)$$

where V is the volume of the unit cell (in $Å^3$), x_c is the atom fraction of activator at which the quenching occurs, the so-called optimum concentration, and N is the number of cations, which can occupy a unit cell. According to our experimental results and the crystal structures of the compounds $MSr_4(BO_3)_3$:Ce^{3+} (M = Li or Na), the values of V, N and x_c are 3341.8 $Å^3$, 16, 0.05 for $LiSr_4(BO_3)_3$ and 3474.7 $Å^3$, 16, 0.09 for $NaSr_4(BO_3)_3$ [9], respectively. The critical distance R_c is found to be about 20 and 16 Å, respectively. It is believed that the concentration quenching of the present compounds is mainly due to the non-radiative transition among the Ce^{3+} ions, which may occur because of the exchange interaction, radiation re-absorption, or multipole–multipole interaction. The exchange interaction is generally responsible for the energy transfer of forbidden transitions and the typical distance is about 5 Å [11]. Because the $5d$–$4f$ transition of Ce^{3+} ion is allowed and the PLE and PL spectra do not overlap (Fig. 3(a) and (b)), the non-radiative transitions among the Ce^{3+} ions take place via electric multipolar interactions according to Dexter theory [21,22].

In the working process of LEDs, especially high-power w-LEDs, the temperature of LED chip increases up to about 200 °C, therefore the thermal stability of phosphor is one of important issues to be considered. A lower thermal quenching effect is in favor of keeping chromaticity and brightness of white light output. Fig. 4 shows the temperature dependences of PL intensities of $MSr_4(BO_3)_3$:Ce^{3+} (M = Li or Na) with optimal composition excited by 355 nm pulse laser. As the increase of temperature, the PL intensity slowly decreases. With heating the phosphor up to 100 °C, the emission intensity remains at about 86% and 73% of that at room temperature for $NaSr_4(BO_3)_3$ and $LiSr_4(BO_3)_3$, respectively, which indicates that phosphor $NaSr_4(BO_3)_3$:Ce^{3+} shows more excellent chemical stability than that of $LiSr_4(BO_3)_3$:Ce^{3+}. As comparison, the curve of PL intensity of BAM depends on the temperature has been published in Ref. [23], and the PL intensity of BAM at 100 °C is decreased to about 85%. And the value is close to the present blue emitting phosphor $NaSr_4(BO_3)_3$:Ce^{3+}. Thus $NaSr_4(BO_3)_3$:Ce^{3+} can serve as a promising phosphor for high power LED application. Generally, the thermal quenching of emission intensity can be explained by configurational coordinate diagram. The excited luminescent center is thermally activated through phonon interaction, and then thermally released through the crossing point between the excited state and the ground state in configurational coordinate diagram. This non-radiative transition probability by thermal activation is strongly dependent on temperature resulting in the decrease of emission intensity [24]. Insets of Fig. 4 show the dependences of PL spectra of $NaSr_4(BO_3)_3$:Ce^{3+} (up) and $LiSr_4(BO_3)_3$:Ce^{3+} (down) on the temperature. It is observed that the emission wavelengths of the Ce^{3+} in the compounds $MSr_4(BO_3)_3$ (M = Li or Na) shift to shorter wavelength with increasing temperature. This blue-shift may be due to the increase of the bond length between luminescent centers and its ligand ions at high temperature, which results in a decreased crystal field and a high-energy shift [23,25].

In order to compare with commercial blue emitting phosphor $BaMgAl_{10}O_{17}$:Eu^{2+} (BAM:Eu^{2+}), Fig. 5 gives the PL (λ_{ex} = 345 nm) spectra of $M_{1+x}Sr_{4-2x}Ce_x(BO_3)_3$ (M = Li or Na) phosphors with optimal composition (x = 0.05 and 0.09 for M = Li and Na, respectively) and the commercial BAM:Eu^{2+} that is currently used as

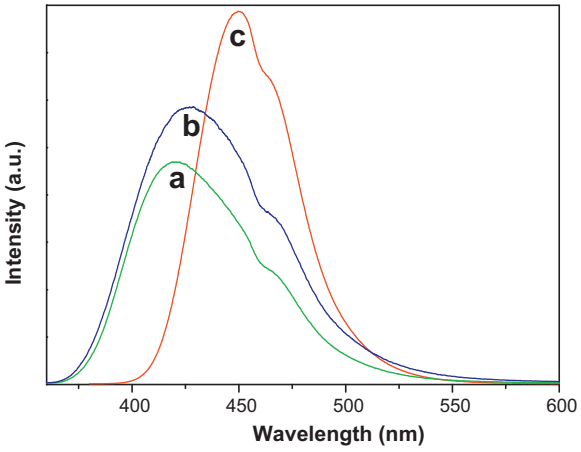

Fig. 5. PL spectra (λ_{ex} = 345 nm) of $Li_{1.05}Sr_{3.9}Ce_{0.05}(BO_3)_3$ (a), $Na_{1.09}Sr_{3.82}Ce_{0.09}(BO_3)_3$ (b) and the commercial blue emitting phosphor BAM.

the blue emitting phosphor for *w*-LEDs based on UV InGaN chip. The integrated emission intensities of $Li_{1.05}Sr_{3.9}Ce_{0.05}(BO_3)_3$ and $Na_{1.09}Sr_{3.82}Ce_{0.09}(BO_3)_3$ are 81% and 107% of the reference BAM. Results indicate that the PL intensities of present blue emitting phosphors are close to that of commercial blue phosphor BAM, and the synthesis temperature is lower at least about 600 °C than that of BAM [7].

4. Conclusions

Novel blue borate phosphors of $M_{1+x}Sr_{4-2x}Ce_x(BO_3)_3$ (M = Li or Na) have been synthesized by using the standard solid-state method. The two optimal compositions are found to be $Li_{1.05}Sr_{3.9}Ce_{0.05}(BO_3)_3$ and $Na_{1.09}Sr_{3.82}Ce_{0.09}(BO_3)_3$. The phosphors show strong broad absorption bands in UV range, and the bright blue emissions are obtained with UV 345 nm as excitation light. The thermal stability of sample $Na_{1.09}Sr_{3.82}Ce_{0.09}(BO_3)_3$ is proved to be higher than that of $Li_{1.05}Sr_{3.9}Ce_{0.05}(BO_3)_3$. On the basis of the above experimental results, it is believed that the present borate phosphors are potential blue emitting phosphor for UV excited *w*-LEDs.

Acknowledgements

The authors wish to thank Analytical and Testing Center of Huazhong University of Science and Technology for providing the facilities to carry out measurements. In addition, National Natural Science Foundation of China (no.50802031) and Ph.D. Programs Foundation of Ministry of Education of China (no.20070487076) support this work. This work was supported in part by Mid-career Researcher Program through NRF grant funded by the MEST (2009-0078682).

References

[1] E.F. Schubert, J.K. Kim, Science 308 (2005) 1274–1278.
[2] K. Shioi, N. Hirosaki, R. Xie, T. Takeda, Y.Q. Li, J. Alloys Compd. 504 (2010) 579–584.
[3] H. He, S. Song, R. Fu, Z. Pan, X. Zhao, Z. Deng, Y. Cao, J. Alloys Compd. 493 (2010) 401–405.
[4] C. Guo, F. Gao, L. Liang, B.C. Choi, J.H. Jeong, J. Alloys Compd. 479 (2009) 607–612.
[5] M.M. Haque, H.I. Lee, D.K. Kim, J. Alloys Compd. 481 (2009) 792–796.
[6] S. Georgescu, A.M. Voiculescu, O. Toma, S. Nastase, C. Matei, M. Osiac, J. Alloys Compd. 507 (2010) 470–474.
[7] S. Ekambaram, K.C. Patil, J. Alloys Compd. 248 (1997) 7–12.
[8] Z. Li, J. Zeng, G. Zhang, Y. Li, J. Solid State Chem. 178 (2005) 3624–3630.
[9] L. Wu, X.L. Chen, H. Li, M. He, Y.P. Xu, X.Z. Li, Inorg. Chem. 44 (2005) 6409–6414.
[10] L.H. Jiang, Y.L. Zhang, C.Y. Li, J.Q. Hao, Q. Su, J. Alloys Compd. 482 (2009) 313–316.
[11] Y. Liu, W. Zhuang, Y. Hu, W. Gao, J. Hao, J. Alloys Compd. 504 (2010) 488–492.
[12] W.H. Chao, R.J. Wu, T.B. Wu, J. Alloys Compd. 506 (2010) 98–102.
[13] L. Liu, R. Xie, N. Hirosaki, Y. Li, T. Takeda, C.N. Zhang, J. Li, X. Sun, J. Am. Ceram. Soc. 93 (2010) 2018–2023.
[14] P. Thiyagarajan, B. Tiwari, M. Kottaisamy, N. Rama, M.S. Ramachandra Rao, Appl. Phys. A 94 (2009) 607–612.
[15] K. Park, J. Kim, P. Kung, S.M. Kim, J. Lumin. 130 (2010) 1292–1294.
[16] Y.Q. Li, N. Hirosaki, R.J. Xie, J. Li, T. Takeda, Y. Yamamoto, M. Mitomo, J. Am. Ceram. Soc. 92 (2009) 2738–2744.
[17] Z. Wang, H. Liang, M. Gong, Q. Su, J. Alloys Compd. 432 (2007) 308–312.
[18] T.W. Kuo, W.R. Liu, T.M. Chen, Opt. Express 18 (2010) 1888–1897.
[19] P. Dorenbos, J. Lumin. 104 (2003) 239–260.
[20] G. Blasse, Philips Res. Rep. 24 (1969) 131–144.
[21] L.G. Van Uitert, J. Electrochem. Soc. 114 (1967) 1048–1053.
[22] D.L. Dexter, J.H. Schulman, J. Chem. Phys. 22 (1954) 1063–1070.
[23] J. Liu, Z. Wu, M. Gong, Appl. Phys. B 93 (2008) 583–587.
[24] J.S. Kim, Y.H. Park, S.M. Kim, J.C. Choi, H.L. Park, Solid State Commun. 133 (2005) 445–448.
[25] V.B. Mikhailik, H. Kraus, D. Wahl, M. Itoh, M. Koike, I.K. Bailiff, Phys. Rev. B 69 (2004) 205110.